


Limnology and diatom ecology of shallow lakes in a rapidly thawing discontinuous permafrost peatland

Kristen A. Coleman ^a, Grace N. Hoskin,^a Laura Chasmer,^b Joshua R. Thienpont,^a William L. Quinton,^c and Jennifer B. Korosi^a

^aFaculty of Environmental and Urban Change, York University, Toronto, Canada; ^bDepartment of Geography and Environment, University of Lethbridge, Lethbridge, Canada; ^cCold Regions Research Centre, Wilfrid Laurier University, Waterloo, Canada

ABSTRACT

Lakes in discontinuous permafrost peatlands are on the front lines of climate change, sensitive to even modest increases in air temperature. The aim of this study was to provide the first limnological characterization of shallow (~1–2 m depth) lakes in the Scotty Creek basin (Northwest Territories, Canada), a field site of circumpolar significance due to the existence of long-term ecohydrological monitoring going back decades. We use this previous work as a foundation to advance our process-based understanding of the potential drivers of lake ecosystem change. Our results showed that dissolved organic carbon (DOC) and lake color were not correlated, a pattern that seems to be an important driver of diatom (siliceous single-celled algae) assemblages in these lakes. Diatoms in the study lakes tended to fall into 1 of 2 assemblage clusters. One cluster, composed of small benthic *Fragilariaceae* and small *Navicula* species (*sensu lato*), was found associated with higher lake color; the second cluster, composed of *Encyonopsis* and large *Navicula* species, was found associated with high DOC, lower color, and the presence of a benthic moss mat. From this finding, we suggest that DOC quality is a primary control on lake ecology in this region for its role in controlling light penetration to the lake bottom. Our hypothesis that the prevalence of nearshore fens and collapse scar wetlands would be important drivers of DOC was not supported in the 9 study lakes with available data to map shoreline features.

ARTICLE HISTORY

Received 27 May 2022

Accepted 31 October 2022

KEYWORDS

channel fens; climate change; collapse scars; DOC; high-resolution data; lake browning

Introduction

Permafrost peatlands cover ~19% of the circumpolar permafrost region (Tarnocai et al. 2009) and contain globally significant stores of terrestrial carbon (Harris et al. 2022). Climate change and an accelerated rate of permafrost thaw have raised concerns about their future role in the global carbon cycle under a warming climate (Hugelius et al. 2020). Shallow lakes are abundant features across many permafrost peatland landscapes of the circumpolar North. They play a critical role in the cycling of water and chemical constituents across the landscape and act as both sentinels and agents of environmental change. Consequently, attempts to decipher the future role of permafrost peatlands in the global carbon balance must include an understanding of how shallow lake ecosystem structure and function are likely to be altered with climate change (Cole et al. 2007).

Discontinuous permafrost landscapes are highly sensitive to even modest warming of air temperatures (Ketles and Tarnocai 1999, Spence et al. 2020). Models project that 40% of the world's permafrost could be

lost by 2100 (SOCR 2021), with sporadic discontinuous permafrost regions potentially permafrost-free by mid-century (Chasmer and Hopkinson 2017). Permafrost thaw can manifest in different ways: it can change the thickness of the seasonally thawed (active) layer, generate a layer of talik separating the underlying permafrost from the overlying active layer, and produce thermokarst terrain (Zhang et al. 1999, 2005, Frey and McClelland 2009). While changes in active layer thickness occur slowly (press disturbance), thermokarst development from the thawing of ice-rich permafrost manifests as a rapid (or pulse) disturbance (Vonk et al. 2015). In southern permafrost peatlands, wetland thermokarst processes typically predominate, resulting in the conversion of forests to wetlands (Quinton et al. 2019).

Wetland thermokarst alters the hydrologic connectivity of the landscape by increasing the number, duration, and depth of flow paths (Smith et al. 2007, Karlsson et al. 2012, Quinton et al. 2019). The hydrological connectivity of a landscape in turn exerts a strong control over transportation of sediment, organic

matter, and nutrients, with shallow lakes playing a critical role in the processing of these materials along hydrological cascades. Increased areal wetland coverage and hydrological connectivity, coupled with increased availability of terrestrial organic matter liberated from thawed soils, has the potential to increase the export of terrestrial organic carbon to lakes. Because terrestrial organic carbon is typically highly colored, increased export of carbon from the catchment can result in a phenomenon known as lake browning (Wauthy et al. 2018), which alters light penetration, thermal regime, and oxygen dynamics in lakes, and can fuel heterotrophic energy pathways in lake food webs (Cole et al. 2006, Porcal et al. 2009, Vonk et al. 2015, Tanentzap et al. 2017).

Increases in lake DOC concentrations are predicted with continued permafrost thaw (Vonk et al. 2013, Wauthy et al. 2018), yet paleolimnological reconstructions of thermokarst lakes have provided mixed results regarding trajectories of lake dissolved organic carbon (DOC) concentrations (Vonk et al. 2012, Bouchard et al. 2013, Thienpont et al. 2013, Coleman et al. 2015), possibly due to, at least in part, localized differences in catchment ecohydrological characteristics. Topography, permafrost extent, ground ice content, surficial geology, and Quaternary history have all been identified as key state factors likely to influence biogeochemical responses of watersheds to permafrost thaw (O'Neill et al. 2019, Vonk et al. 2019, Tank et al. 2020). Consequently, representation across broad geographic gradients is required to disentangle the trajectories and drivers of limnological change in northern lakes and make predictions at the circumpolar scale. Even within regions, responses of permafrost peatlands to warming can be variable, highlighting the need to better understand the processes underlying ecosystem change (Sim et al. 2021). In this study, we contribute to addressing these knowledge gaps by providing the first limnological characterization of small shallow lakes in the Scotty Creek basin of the southwestern Northwest Territories (Canada).

The Scotty Creek basin (61°180N, 121°180W) is a region of low relief and extensive peatlands located at the northern extent of the sporadic discontinuous permafrost zone in the Taiga Plains Ecozone. Here, permafrost exists beneath treed peat plateaus while surrounding wetlands, including channel fens and collapse scar wetlands (hereafter “collapse scars”), are predominately treeless and permafrost-free. Warming air temperature, which has accelerated since ~1970, has resulted in the rapid loss of permafrost (Quinton et al. 2019). The region is predicted to be permafrost-free by mid-century (Chasmer and Hopkinson 2017).

The Scotty Creek Research Station has supported intensive field, remote sensing, and modeling studies since the late ~1990s, providing a long-term perspective on thaw-induced watershed changes rarely available for remote subarctic regions (Quinton et al. 2019). To date, however, little research has been conducted on the many small lakes and ponds found within the Scotty Creek basin. In a recent comparison of hydrological trends in 32 circumpolar peatland basins, the Taiga Plains were unique in experiencing a widespread increase in annual basin runoff in the absence of increasing precipitation (Mack et al. 2021), a phenomenon linked to accelerated wetland thermokarst (Connon et al. 2014). Clearly, the Scotty Creek basin is in a period of rapid transition, where limnological research should be prioritized.

The objectives of this study were to (1) document the present-day limnology of shallow lakes in the Scotty Creek basin as a benchmark from which to examine future limnological change, and (2) examine spatial relationships among water chemistry, near-shore landscape characteristics, and diatom (siliceous algae) assemblages to understand controls on limnological characteristics and make predictions about drivers of future change. To meet our objectives, we analyzed surface water chemistry and sedimentary diatom assemblages in 16 lakes in or near the Scotty Creek basin and used high-resolution aerial imagery available for 9 of the lakes to map channel fen and collapse scar areas within 250 m of the lake perimeter. We also collected high-resolution logger data for depth, oxygen, light, and temperature profiles over the 2019 ice-free season in 2 lakes in the Scotty Creek basin, which we propose as candidate sites to establish a long-term lake monitoring program. Overall, this study provides a foundation for advancing our process-based understanding of the drivers of limnological change in rapidly thawing discontinuous permafrost peatlands.

Methods

Overview

We chose 16 lakes to sample water chemistry and sedimentary diatom assemblages because they are close to one another and centered on the Scotty Creek basin, allowing us to explore the range of limnological variability within a small geographic area (Fig. 1). Of the 16 lakes, 8 were within the Scotty Creek basin, an additional 6 were just outside the boundaries of the Scotty Creek watershed, and 2 (FS1 and FS2) were northeast of Scotty Creek. FS1 and FS2 were slightly larger and

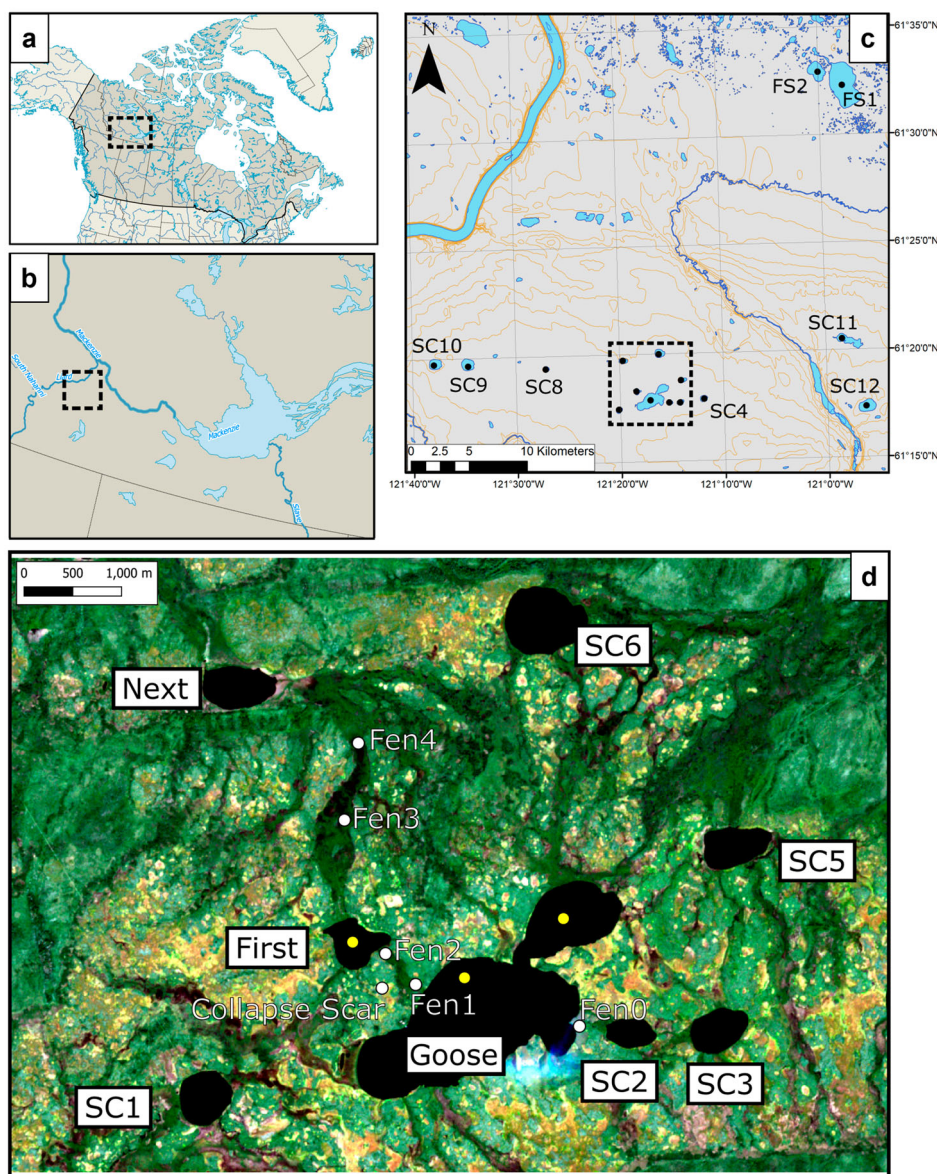


Figure 1. Study area: Scotty Creek Basin, Northwest Territories, Canada. (a) Approximate location of the site within Canada; (b) approximate location of the site within Taiga Plains ecozone; (c) location of all study lakes; (d) true color image using Sentinel 2A data (accessed June 2021) of study lakes highlighted in (c) and includes wetland sample sites (white dots). Yellow markers are locations of data loggers.

in a more fluvially influenced catchment setting than the other lakes.

For 9 of the 16 study lakes, including SC8 and the 8 lakes within the Scotty Creek basin, we used previously available landscape classification data (Chasmer et al. 2014) to quantify the area within 250 m of the lake shoreline composed of fens and collapse scars. We used the landscape classification data to explore relationships between water chemistry, diatoms, and land cover. Two of the lakes within the Scotty Creek basin (First Lake and Goose Lake) are easily accessible from the Scotty Creek Field Station, which allowed us to conduct more intensive field

sampling. For these lakes, we deployed loggers and collected water and sediments from adjacent wetlands to further refine our understanding of their limnology.

Field methods

The 16 lakes were sampled from the center of the lake by helicopter in mid-July 2018 (Fig. 1). That season, ice-off occurred 4–10 May 2018. Conductivity and pH were measured at all sites in situ using a Hanna multiprobe, but oxygen measurements were not recorded because of equipment malfunction. Lake depths were measured

using an acoustic depth sounder; however, depths were not used in statistical analyses because the interference of dense moss mats and macrophytes established on many lake bottoms prevented stabilized readings of the depth sounder. For many lakes, readings fluctuated by tens of centimeters, which is significant for these shallow systems. For all sites, water samples were collected in 2 pre-sterilized 1 L polyethylene bottles. We filtered 1 L through 0.45 µm cellulose acetate filters within 24 h of collection for analysis of DOC and total dissolved nitrogen (TDN). Unfiltered water was poured into 250 mL glass bottles containing 0.5 mL nitric acid, including a field blank using deionized (DI) water, and sent to SGS Laboratories (Montreal, QC, Canada) for elemental analysis. Sediment cores were collected from the 16 lakes using a Uwitec gravity corer (UWITEC, Mondsee, Austria) with an internal diameter of 8.6 cm and sectioned into 0.5 cm intervals using a modified Glew (1988) extruder. The top 0.5 cm of each core was used for the analysis of modern diatom assemblages. Based on ^{210}Pb dating, the top 0.5 cm represented ~2–5 years of sediment accumulation in these lakes (Coleman and Korosi 2023).

In June 2019, surface water and sediments were sampled from Goose Lake and First Lake at the Scotty Creek Research Station as well as 5 fen sites and 1 collapse scar site (Fig. 1d). Additionally, substrate samples (submerged vegetation, submerged peat, sediment, and grasses) were collected from shoreline environments around Goose Lake and from a benthic moss mat in the center of the north basin of Goose Lake at a water depth of ~1 m. Water and sediment sampling followed the same methods used for the 2018 sampling of the 16 lakes described earlier, except that we were able to collect dissolved oxygen (DO) data with the Hanna Multiprobe (Hanna Instruments, hannainst.com).

Buoys equipped with HOBO Pendant wireless temperature and light data loggers, Onset HOBO U26 DO data loggers, and Onset HOBO U20 depth loggers (onsetcomp.com) were deployed in both the main basin and northern basin of Goose Lake and center of First Lake (Fig. 1d) on 7 June (~1 month past ice-off) and removed 22 August 2019. Each buoy was connected to a rope anchored to the sediment with 20 lb weights. An additional rope was suspended from the buoy with 3 temperature/light loggers and 1 oxygen logger attached. The depth logger was attached to the weight to keep it stationary in the water column in relation to the sediments and was kept afloat using empty 2 L bottles. Precipitation data were collected using a Pluvio totalizing station, located at the Scotty Creek Research Station adjacent to Goose Lake, and corrected for undercatch. Precipitation was recorded every 30 min

to examine the impact of precipitation on other time-series data (e.g., light and depth).

Laboratory analysis of water chemistry

DOC and TDN were analyzed on a Shimadzu-TOC5000 Series TOC-L analyzer (shimadzu.com) following the combustion catalytic oxidation method and non-dispersive infrared detection. Standards were made using potassium hydrogen phthalate for instrument calibration and performance, and then acidified using HCl and sparged to purge dissolved inorganic carbon (DIC). True color was measured using the platinum-cobalt method on a Genesys 10S UV-Vis spectrophotometer (Thermo Fisher Scientific, Waltham, MA, USA; APHA 2011). Alkalinity was analyzed by titrating samples with 0.02N H_2SO_4 (APHA 1998). Samples were sent to SGS Laboratories for elemental analysis, including total phosphorus (TP), using Inductively Coupled Plasma Mass Spectrometry (ICP-MS) and Inductively Coupled Plasma Optical Emission Spectroscopy (ICP-OES). Although perchloric acid digestion followed by colorimetry is more common for analysis of TP, close agreement has been found between this method and ICP-MS (Ivanov et al. 2012), as used here.

Physical landscape characterization

Shoreline development and lake area

The shoreline development ratio (D_L), an index that describes how close a lake is to a perfect circle, was calculated for all 16 study lakes. Lakes with a D_L close to 1 have circular shapes while lakes with high D_L have more jagged and crenulated shapes. D_L is the ratio of the perimeter of the lake to the perimeter of a circle with the same area:

$$D_L = S_L / [2 \cdot (\pi \cdot A_o)^{0.5}], \quad (1)$$

where S_L is shoreline length and A_o is the surface area of the lake. Lakes with a higher D_L have higher potential to develop littoral communities and increase the exposure of lakes to the surrounding shorelines. Lake area and perimeter were calculated using the polygon function in Google Earth.

Buffer and overlay landscape analysis

Nine of the 16 study lakes were used for the buffer and overlay landscape analysis. Buffering is the process of creating an output polygon layer that delineates a zone of specified width around a feature of interest. An overlay is the process of taking 2 or more different maps of the same area and placing them on top of one

another. In this study, we applied a 250 m buffer around the perimeter of the 9 study lakes, followed by an overlay analysis to determine how much fen and collapse scar area fell within each buffer. The output layers included only shapefiles of the collapse scars and fens that overlapped within the 250 m buffer. The buffer and overlay analyses were done in ArcMap 10.7.1 using a raster file of the Scotty Creek study area. Individual shapefiles were created for each land classification (channel fen, collapse scars, water, moraine/upland, and permafrost), and the water layer was separated into individual lakes.

Subfossil diatom analysis

Diatom slides were prepared following Battarbee et al. (2001) using the hydrogen peroxide method and mounted using Naphrax (Brunel Microscopes Ltd, Chippenham, UK). Diatom valves were identified using an Amscope B690C-PL microscope (amscope.com), multiple reference texts (Krammer and Lange-Bertalot 1997, 1999, 2000, Fallu et al. 2002), and online databases (Guiry and Guiry 2021, Spaulding et al. 2021). Between 300–500 valves were counted per site, except for Fen 4 and the collapse scar site with markedly low diversity (Hill's $N_2 < 4$), where a minimum of 175 valves were counted. Diatom species were grouped based on similar ecologies (Supplemental Table S1) and were displayed as relative abundances. Chrysophyte cysts, which can form in response to changing environmental conditions, and protozoan plates, which can provide information on moisture levels, were also present on diatom slides and enumerated and displayed on figures as percentages relative to the sum of all diatom valves.

Data analysis

Data retrieved from data loggers were plotted using the *ggplot* package (Wickham et al. 2019) in R (R Core Team 2020). The percentage of light absorption per cm (a) was calculated by the equation:

$$a = 100 \left(\frac{I_0 - I_z}{I_0} \right) / z, \quad (2)$$

where I_0 is the irradiance recorded in the shallowest sensor and I_z is the irradiance recorded in the deepest sensor divided by the depth (cm) between the 2 sensors. We removed anomalous negative values caused by higher irradiance values recorded by the deeper sensor than by the shallower sensor, likely a result of shading of the shallower sensor by the buoy. A LOESS smoothed

line was included in the figures using the *stat_smooth* function in *ggplot* in R.

Water chemistry variables with concentrations below detection were not included in any statistical analyses (mercury, silver, arsenic, beryllium, boron, bismuth, molybdenum, nickel, antimony, selenium, tin, thallium, zirconium, and zinc). Variables were also removed if we found evidence of contamination based on anomalously high field blank concentrations (aluminum, cadmium, cobalt, chromium, copper, iron, lead, titanium, uranium, and vanadium). Spearman's correlation analyses, used here because of the non-normal distribution of most variables, were calculated on remaining water chemistry variables to determine any statistically significant relationships between water chemistry variables and A_o or D_L . Water chemistry variables included in the Spearman's correlation analyses included pH, DOC, TDN, true color (color), phosphorus (TP), conductivity, alkalinity, calcium (Ca), potassium (K), lithium (Li), magnesium (Mg), manganese (Mn), sodium (Na), silicon (Si), and strontium (Sr).

Principal components analysis (PCA) was used to visualize limnological variation among lakes. Variables were standardized using the *scale* function in the *vegan* package (Oksanen et al. 2019) in R. A PCA was generated for all 16 lakes to examine variation between lakes with respect to A_o , D_L , pH, DOC, TDN, color, conductivity, Li, and Mn. A_o and D_L were plotted passively. Highly correlated variables were removed from the PCA. For example, conductivity was correlated with alkalinity, calcium (Ca), potassium (K), magnesium (Mg), and strontium (Sr). The remaining variables were selected based on their importance in structuring biological communities (pH, DOC, TDN, TP, color, and conductivity), usefulness as a lithogenic tracer (Li), or sensitivity to redox conditions (Mn). Li, TP, and A_o were normalized using a log transformation, and D_L and conductivity were normalized using a log-log transformation. The remaining variables were already normally distributed, and no transformation was applied. A PCA was also generated for the subset of 9 lakes used in landscape analyses to visually examine relationships between the same water chemistry variables described earlier and collapse scar or fen coverage within 250 m of the lake perimeter. Collapse scar and fen coverage were plotted passively, and Mn was normalized using a log transformation.

Direct ordination (redundancy analysis [RDA]) was used to evaluate relationships between diatom community composition and environmental variables. Lake area and conductivity were log transformed to

normalize distribution, and species data were Hellinger transformed to standardize species assemblage data from absolute to relative values. A variance inflation factor (VIF) test was run to assess multicollinearity. Variables with high VIFs were sequentially removed from analysis until all environmental variables had VIFs <10. Variables retained in the analysis were pH, color, DOC, area, and conductivity. Significance of the RDA was determined using an ANOVA-like permutation test. Correlation analyses were conducted using the *Hmisc* package (Harrell 2021), and PCAs, VIFs, RDAs, and permutation tests were conducted using the *vegan* package (Oksanen et al. 2019) in R.

Results

High-resolution assessment of Goose Lake and First Lake

Depth measurements obtained from depth loggers deployed in First Lake and the 2 main basins of Goose Lake (Fig. 1d) from 7 June to 22 August showed close agreement among all 3 loggers, suggesting water levels of these shallow (~1 m) lakes fluctuated by ~30–40 cm throughout this period (Fig. 2a–c). Water levels fluctuated through June and July and began to stabilize towards the end of the recorded period, with the lowest levels occurring in early to mid-June and mid-July. Bottom DO measurements ranged from 5 to 12.5 mg/L in Goose Lake, in both the north basin (Fig. 2a) and the main basin (Fig. 2b). In First Lake, DO dropped to zero for periods of time, likely a result of the logger dropping into the sediments during periods of lower water levels (Fig. 2c).

The consistency between temperature readings at different depths indicated that the entire water column in both lakes was mixed throughout the recorded period (Fig. 2). Temperature measurements were consistent between lakes and fluctuated between 10 and 25 °C throughout the recorded period. All lakes recorded warmer periods in mid-June and late July/early August. The calculated % absorption of light per cm was similar between Goose Lake and First Lake, and although light penetration fluctuated through time, no clear seasonal trends were apparent (Fig. 2). In Goose Lake, however, periods of higher light absorption (e.g., in late July) coincided with warmer temperatures (Fig. 2a–b). Rainfall events occurred sporadically throughout the season, with the largest rainfall event occurring on 18 July when 12.4 mm of rain fell in an hour. Lake depth increased by ~20 cm in Goose Lake and First Lake after this rainfall event, and maximum depth occurred on 23 July (Fig. 2).

Characterization of lakes in or near the Scotty Creek basin

Morphology and water chemistry of the 16 lakes

In 2018, lake depths of the 16 surveyed lakes ranged from ~0.9 to 2.1 m, but dense macrophyte stands or benthic moss mats likely interfered with sonar measurements; measurement readings in some lakes did not stabilize and fluctuated by tens of centimeters. Lake area ranged from 11 to 244 ha, except for a notably larger lake (FS1) of 713 ha (Table 1). Lakes were circumneutral to slightly alkaline (pH = 7.85–8.75). Alkalinity ranged from 28 to 124 mg/L CaCO₃, conductivity from 55.5 to 244.2 µS/cm, DOC from 12.96 to 23.74 mg/L, and water color from 18 to 463 TCU (Table 1). TDN ranged from 0.54 to 1.54 mg/L and TP from 8 to 38 µg/L.

Near-shore landscape characterization of nine selected thermokarst lakes

Landscape coverage of fen environments varied between 0% and 34% within 250 m of the perimeters of the 9 lakes included in the landscape characterization analyses. Collapse scars were more extensive, covering 13.4–48.9% of the landscape within 250 m of the lake perimeters (Fig. 3). Lakes were generally well connected through channel fen networks, except for SC5 and SC8, which were more isolated. SC8 had no fen environment within 250 m of the lake, indicating it may be hydrologically isolated, and although SC5 had a fen-like environment containing grasses and sedges along the western edge of its shoreline, it was not hydrologically connected to a channel fen network (Fig. 3).

Water chemistry of wetland environments near Goose and First lakes

The 5 fen environments had lower pH ranges than sampled lakes, being circumneutral to slightly acidic (5.97–7.40), and had higher DOC concentrations than lakes, ranging from 23.08 to 33.7 mg/L. Compared to this study, Gordon et al. (2016) previously reported lower pH values (5.15–5.46) and higher DOC values (~42–49 mg/L) for fens in the Scotty Creek basin. Water color ranged from 54 to 459 TCU, alkalinity from 26 to 50 mg/L CaCO₃, TN from 0.52 to 0.91 mg/L, and conductivity from 25 to 82 µS/cm. DO ranged from 2.06 to 9.27 mg/L (or 17.6–89.7% saturation) and was slightly lower than recorded by data loggers in Goose Lake and First Lake. The one collapse scar sampled had high DOC (46.8 mg/L), which was in range of values reported by Gordon et al. (2016), and also high color (522 TCU), low pH (5.33), low alkalinity (4 mg/L CaCO₃), and low conductivity (25 µS/cm).

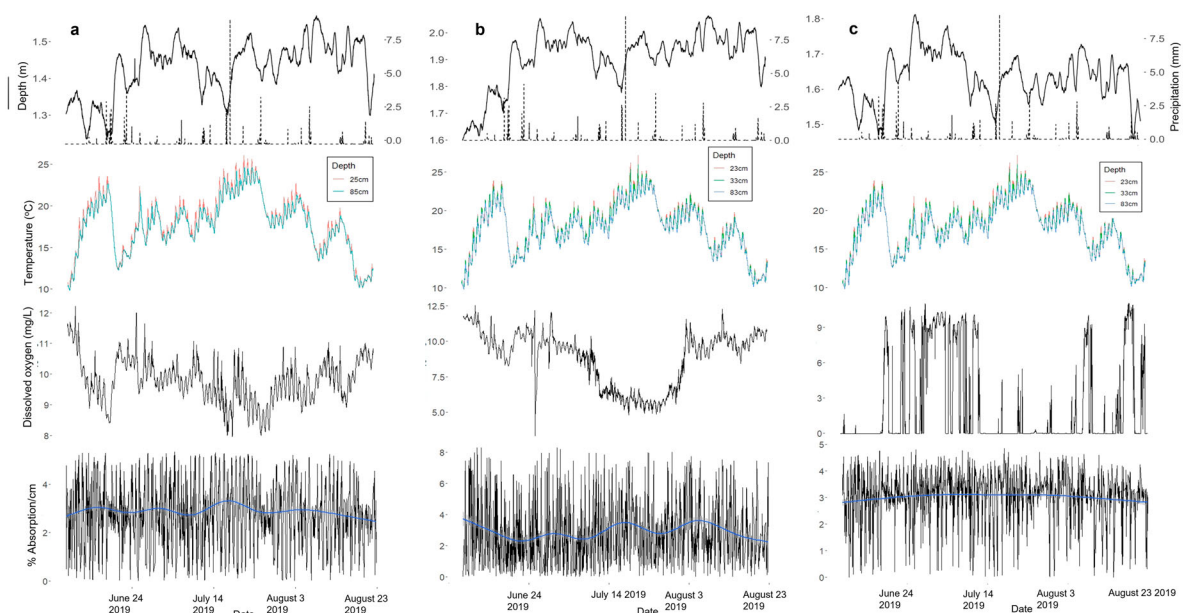


Figure 2. Lake depth, temperature, dissolved oxygen, and light absorption recorded every 30 min from 7 June to 22 August 2019 from Goose Lake's north basin (a), Goose Lake's main basin (b), and First Lake (c). Precipitation data were recorded from a Pluvio totalizing station located near Goose Lake.

TDN (0.59 mg/L) and DO (6.35 mg/L; 58.5% saturation) were within the range of water chemistry variables measured in the 5 fen environments.

Analysis of relationships between water chemistry and landscape features

PCA axis 1 explained 50% of the variation in water chemistry in the 16-lake dataset, largely driven by conductivity, lithium (Li), manganese (Mn), TDN, and color, whereas PCA axis 2 explained 23% of the

variation in the dataset, largely driven by DOC and TP (Fig. 4a). Generally, lakes were well dispersed throughout the ordination space; however, SC3, SC8, SC1, SC2, Next Lake, SC4, SC9, and SC11 were well dispersed along PCA axis 2 but not axis 1, indicating these lakes differed in water chemistry variables associated with axis 2 (DOC and TP). Some lakes seemed to have similar water chemistry (e.g., SC2 and Next Lake; Fig. 4a), despite being relatively distant (Fig. 1). PCA ordination of the 9-lake dataset (Fig. 4b) illustrated the relationship between the same water chemistry variables examined earlier (Fig. 4a) and proportion of collapse scar and fen environments within 250 m of lakes. Here, PCA axis 1 explained 46% of the variation in the dataset and was driven by conductivity, Mn, TN, Li, and TP, whereas PCA axis 2 explained 21% of the dataset and was driven by pH, color, and DOC (Fig. 4b).

Correlation analyses suggested that lake area in this region was strongly ($r > 0.6$) and positively correlated to conductivity; ($r = 0.79$, $p < 0.01$); alkalinity ($r = 0.85$, $p < 0.01$); major ions such as Ca ($r = 0.74$, $p < 0.01$), Mg ($r = 0.77$, $p < 0.01$), and K ($r = 0.78$, $p < 0.01$); and moderately ($0.3 > r > 0.6$) and positively correlated with TDN ($r = 0.54$, $p < 0.05$), Mn ($r = 0.53$, $p < 0.05$), and Sr ($r = 0.57$, $p < 0.05$) (Table 2). Lake area was also found to be strongly and negatively correlated to color ($r = -0.85$, $p < 0.01$; Table 2). Shoreline development index was moderately and positively correlated with conductivity ($r = 0.50$, $p < 0.05$) and Mg

Table 1. Physical characteristics and modern water chemistry statistics for 16 lakes in the Scotty Creek and surrounding basins, collected July 2018.

	Mean	SD	Min	Max	Median
Depth (m)	1.3	0.4	0.9	2.1	1.2
Area (km ²)	1.06	1.69	0.11	7.13	0.32
Shoreline development index	1.18	0.21	1.02	1.75	1.09
pH	8.23	0.27	7.85	8.75	8.20
DOC (mg/L)	18.79	3.13	12.96	23.74	18.35
True color (TCU)	176	124	18	463	174
TP (µg/L) (unfiltered)	18.3	7.9	8.0	38.0	17.0
TDN (mg/L) (filtered)	0.90	0.28	0.54	1.54	0.79
Conductivity (µS/cm)	106.9	58.5	55.5	244.2	83.1
Alkalinity (CaCO ₃) (mg/L)	54	29	28	124	43
Calcium (mg/L)	15.4	6.5	7.9	29.8	13.3
Potassium (mg/L)	0.61	0.65	0.19	2.49	0.34
Lithium (µg/L)	1.4	0.8	0.7	3.2	1.2
Magnesium (mg/L)	4.67	3.08	2.24	12.70	3.51
Manganese (µg/L)	17.3	8.3	4.9	35.1	15.5
Sodium (mg/L)	2.35	1.93	0.74	7.25	1.62
Silicon (mg/L)	1.52	0.98	0.27	4.33	1.21
Strontium (µg/L)	61.1	36.0	28.5	149.0	45.3

SD = standard deviation; Area = surface area; DOC = dissolved organic carbon.

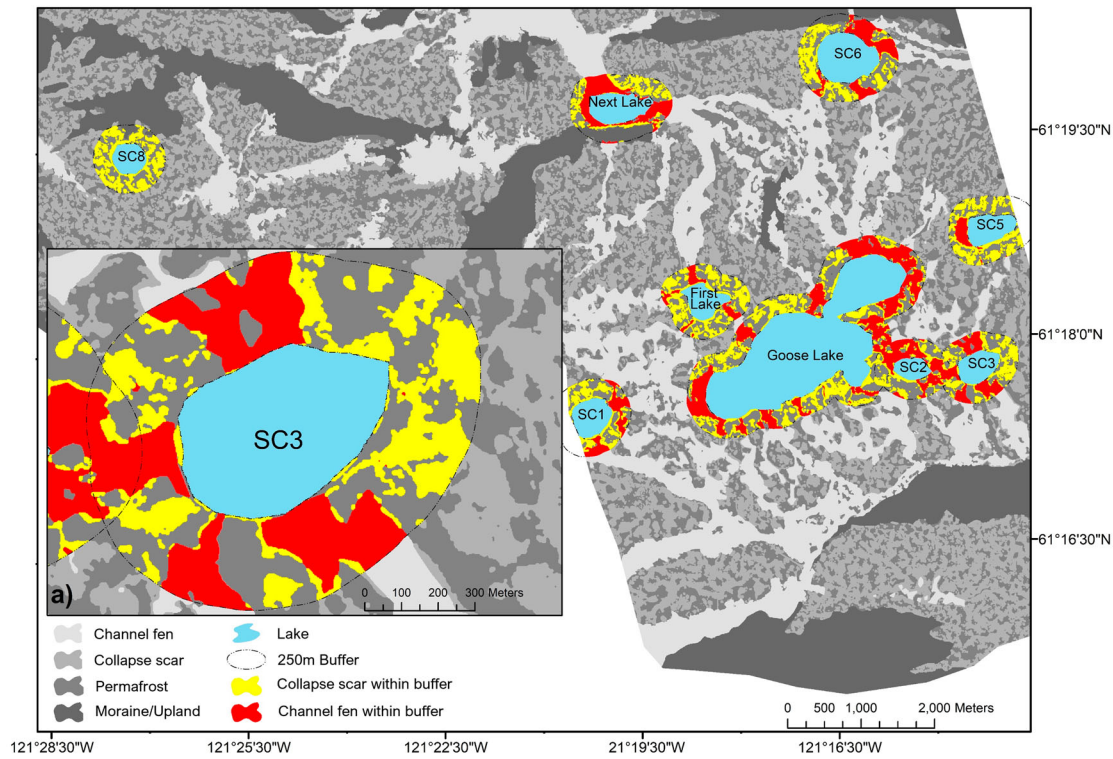


Figure 3. Land classifications of the Scotty Creek basin based on those established in Chasmer et al. (2014). The 250 m buffer zones show bog (red) and fen (yellow) environments within the buffer zones. Inset is a detailed example of the 250 m buffer zone around lake SC3.

($r = 0.48$, $p < 0.05$; Table 2). DOC was moderately and positively correlated to both TN ($r = 0.52$, $p < 0.05$) and TP ($r = 0.58$, $p < 0.05$; Table 2). TDN was not significantly correlated to TP ($r = 0.48$, $p > 0.05$; Table 2). Color was moderately and negatively correlated to pH

($r = -0.54$, $p < 0.05$) and strongly and negatively related to TDN ($r = 0.69$, $p < 0.01$), whereas TDN was moderately and positively related to Li ($r = 0.50$, $p < 0.05$; Table 2). DOC and color were not correlated in these lakes ($r = 0.16$, $p = 0.55$; Table 2).

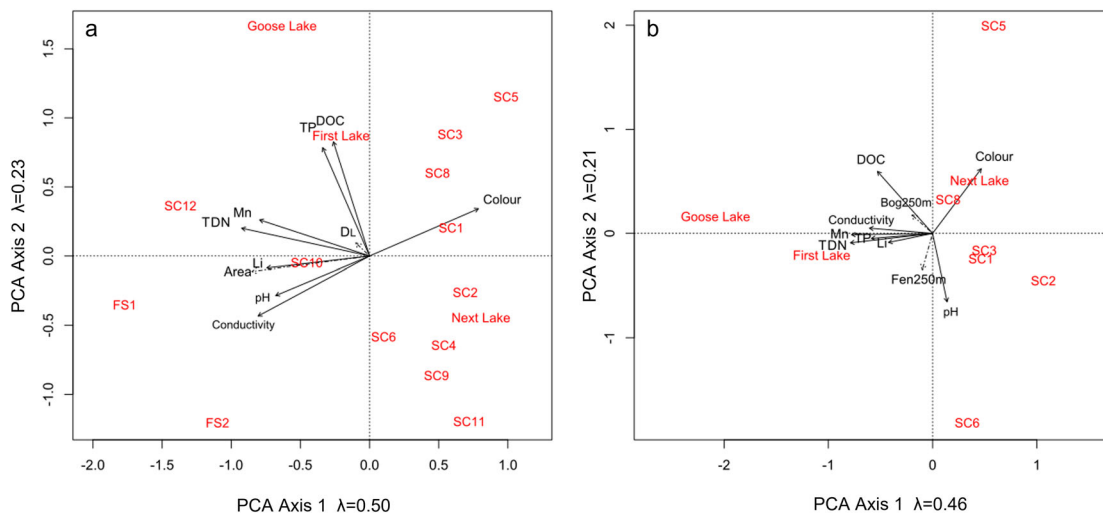


Figure 4. (a) Principal components analysis (PCA) of select water chemistry variables and physical characteristics of 16 shallow lakes in the Scotty Creek basin and (b) select water chemistry variables and proportion of collapse scar (Bog250 m) and fen (Fen250 m) environments within 250 m of lake shorelines for 9 lakes included in landscape classification analyses. Dashed lines represent variables plotted passively. A_0 = lake area, D_L = shoreline development index.

Table 2. Spearman's correlation coefficients of water chemistry variables and physical lake characteristics for 16 lakes in the Scotty Creek basin.

	A _o	D _L	pH	DOC	TP	TDN	Color	Cond	Alk	Ca	K	Li	Mg	Mn	Na	Sr
A _o	1.00	0.45	0.21	-0.06	-0.07	0.54	-0.85**	0.79**	0.85**	0.74**	0.78**	0.29	0.77**	0.52	0.36	0.57*
D _L		1.00	-0.07	0.12	-0.19	0.22	-0.23	0.50*	0.47	0.43	0.35	0.35	0.48	0.12	0.30	0.42
pH			1.00	-0.16	0.10	0.45	-0.54	0.48	0.46	0.37	0.63**	0.16	0.51*	0.48	0.42	0.49
DOC				1.00	0.58*	0.52*	0.16	-0.01	-0.06	-0.01	-0.06	0.17	-0.04	0.22	-0.02	-0.04
TP					1.00	-0.06	-0.21	-0.11	-0.28	-0.05	0.20	-0.20	0.51*	0.29	-0.21	0.58*
TDN						1.00	-0.69**	0.53	0.52*	0.49	0.65**	0.50*	0.51*	0.52*	0.53*	0.58*
Color							1.00	-0.81**	-0.68**	-0.84**	-0.38	-0.74**	-0.54*	-0.55*	-0.65**	0.57**
Cond								0.94**	0.95**	0.83**	0.32	0.99**	0.54*	0.33	0.80**	0.76**
Alk									1.00	0.85**	0.32	0.36	0.95**	0.57*	0.48	0.86**
Ca										1.00	0.74**	0.37	0.94**	0.47	0.28	0.86**
K											1.00	0.19	0.43	0.44	0.75**	0.55*
Li												1.00	0.29	0.29	0.82**	0.55*
Mg													1.00	0.37	0.77**	0.55*
Mn														1.00	0.29	0.51*
Na															1.00	0.51*
Sr																1.00

* $p < 0.05$, ** $p < 0.01$.A_o = surface area; D_L = shoreline development index; DOC = dissolved organic carbon; TP = total phosphorus; TDN = total dissolved nitrogen; Color = true color; Cond = conductivity; Alk = alkalinity; Ca = calcium; K = potassium; Li = lithium; Mg = magnesium; Mn = manganese; Na = sodium; Sr = strontium.

Diatom communities

Lakes

With a few exceptions, 2 common diatom assemblages were identified in the small lakes within the Scotty Creek basin and surrounding areas. The first assemblage, identified in SC9, SC3, SC2, SC1, SC5, and SC11, was dominated by small benthic *Fragilariaceae* (mainly *Pseudostaurosira brevistriata*, *P. parasitica*, *Staurosira construens*, and *S. venter*) and small *Navicula* species sensu lato, including *Sellaphora nigri*, and *Sellaphora seminulum* (Fig. 5). The second assemblage, identified in SC4, SC6, SC12, Next Lake, FS2, Goose Lake, and SC10, was dominated by *Encyonopsis* spp. (*E. cesatii* and *E. descripta*), and large *Navicula* spp. (*N. cryptocephala*, *N. cryptotenella*, and *N. radiosa*). Many of these lakes (SC12, Goose Lake, SC10, Next Lake, and FS2) also had high abundances of *Brachysira* spp. (*B. styriaca*, *B. vitrea*, and *B. zellensis*; Fig. 5). Some exceptions occurred in these common groupings: The assemblage in FS1 was dominated by *Achnanthes minutissimum*; the assemblage in SC8 was dominated by *A. minutissimum*, large *Navicula* spp., *Nitzschia* spp., and *Brachysira* spp.; and the assemblage in First Lake was dominated by *A. minutissimum*, large *Navicula* spp., *Nitzschia* spp. (mainly *N. fonticola* and *N. palea*), and centric planktonic species (*Lindavia michiganiana* and *Discostella pseudostelligera*; Fig. 5). The abundance of chrysophyte cysts relative to diatom valves was variable, ranging from 0% to ~20%. Higher abundances were found in SC3 (~20%) and SC11 (~19%) and absent in FS1 and SC9. Protozoan plates were present in low abundance in most lakes (~0.2–4.6%) and absent in SC9 and SC10 (Fig. 5).

RDA of diatom assemblages and pH, color, DOC, lake area, and conductivity was statistically significant ($F = 1.8422$, $p < 0.05$). The selected variables collectively explained 47.9% of the variance in the diatom assemblages, 40% of which was explained in the first 2 RDA axes (Fig. 6). Some species preferences were identified in the RDA. For example, *B. vitrea* was associated with lakes with greater surface area. *N. cryptocephala*, *N. radiosa*, *E. cesatii*, *E. descripta*, *Kobayasiella jaagi*, *Cymboplectura incerta*, and *B. styriaca* were all associated with lakes with higher DOC, whereas *S. construens*, *S. venter*, and *P. brevistriata* were associated with high color. Lakes SC1, SC2, SC3, SC5, and SC9 had a similar diatom assemblage, whereas Next Lake, Goose Lake, and lakes SC4, SC6, SC10, and SC12 had similar assemblages. FS2, SC8, and First Lake also had a similar assemblage (Fig. 6).

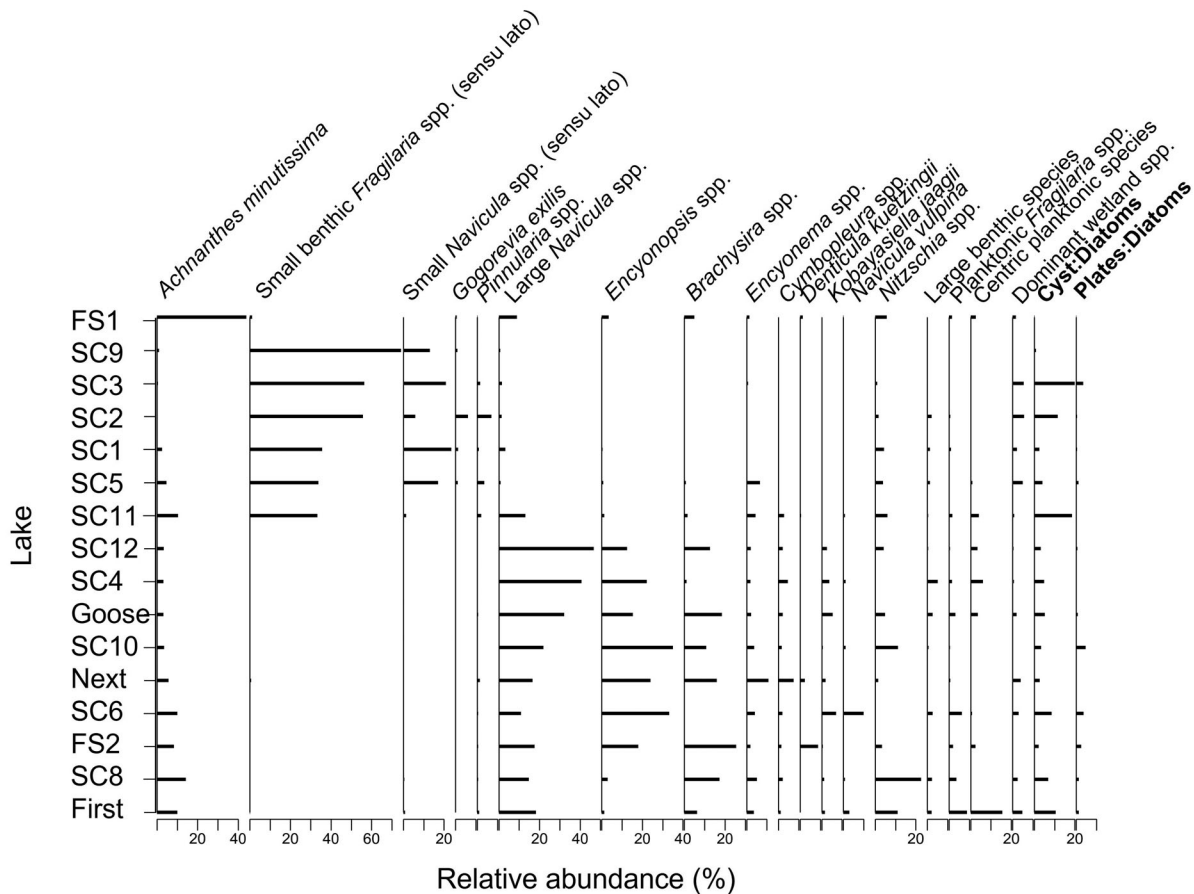


Figure 5. Relative abundance diagram displaying the most common diatom taxa in the modern sediments retrieved from 16 shallow lakes in the Scotty Creek and neighboring basins. Species were grouped based on similar ecology. Species or ecological groups present at <2% relative abundance are not shown. Lakes were ordered using diatom PCA axes scores. Ratio of chrysophyte cysts to diatom valves and protozoan plates to diatom valves are also displayed.

Wetland diatom assemblages

Diatom assemblages identified in the wetland samples were variable but exhibited notable differences from lake diatom assemblages. The most abundant diatoms found in fen environments were *Eunotia* spp. (mainly *E. bilunaris* and *E. subarcuatooides*), *Gomphonema* spp. (mainly *G. parvulum*), and *Tabellaria* spp. Also present were *Rossethidium pusillum*, *A. minutissimum* (Fig. 7), *Nitzschia* spp. (mainly *N. fonticola* and *N. palea*), large *Navicula* spp. (mainly *N. cryptocephala*, *N. cryptotenella*, and *N. radiosa*), *Kobayasiella subtilissima*, and planktonic *Fragilaria* (mainly *F. tenera*) spp. (Fig. 7). The relative abundances of chrysophyte cysts (7–36%) and protozoan plates were variable (2–37%) but generally higher in fens than lakes (Fig. 7). The diatom assemblage in the collapse scar sample was dominated by *K. subtilissima* (95%). The highest relative abundances of both chrysophyte cysts and protozoan plates were found in the collapse scar sample (both at 42% relative abundance; Fig. 7).

Diatom assemblages identified in lake substrate samples

In the lake substrate samples, *Tabellaria* spp. and large *Navicula* spp. (mainly *N. cryptocephala*, *N. cryptotenella*, and *N. radiosa*) were the most abundant diatom species identified. *Tabellaria* spp. was present in high abundances in grass (~48%) and submerged vegetation (~71%) samples and also present in the submerged peat sample (~11%; Table 3). Large *Navicula* spp. were found in high abundance in the sediment (~38%), submerged peat (~30%), and benthic moss mat (~39%) samples (Table 3). In addition to the large *Navicula* spp., the diatom assemblage identified in the sediment sample also consisted of planktonic *Fragilaria* spp. (mostly *F. tenera*), *Encyonema* spp. (mostly *E. silesiacum*), and *Brachysira* spp. (*B. styriaca* and *B. vitrea*; Table 3). The submerged peat sample also contained planktonic *Fragilaria* species and *Encyonopsis* species (*E. descripta* and *E. cesatii*). In addition to *Tabellaria* spp. the grass sample also consisted of *Gomphonema* spp. (mostly *G. parvulum*) and *A. minutissimum* while the benthic moss mat sample

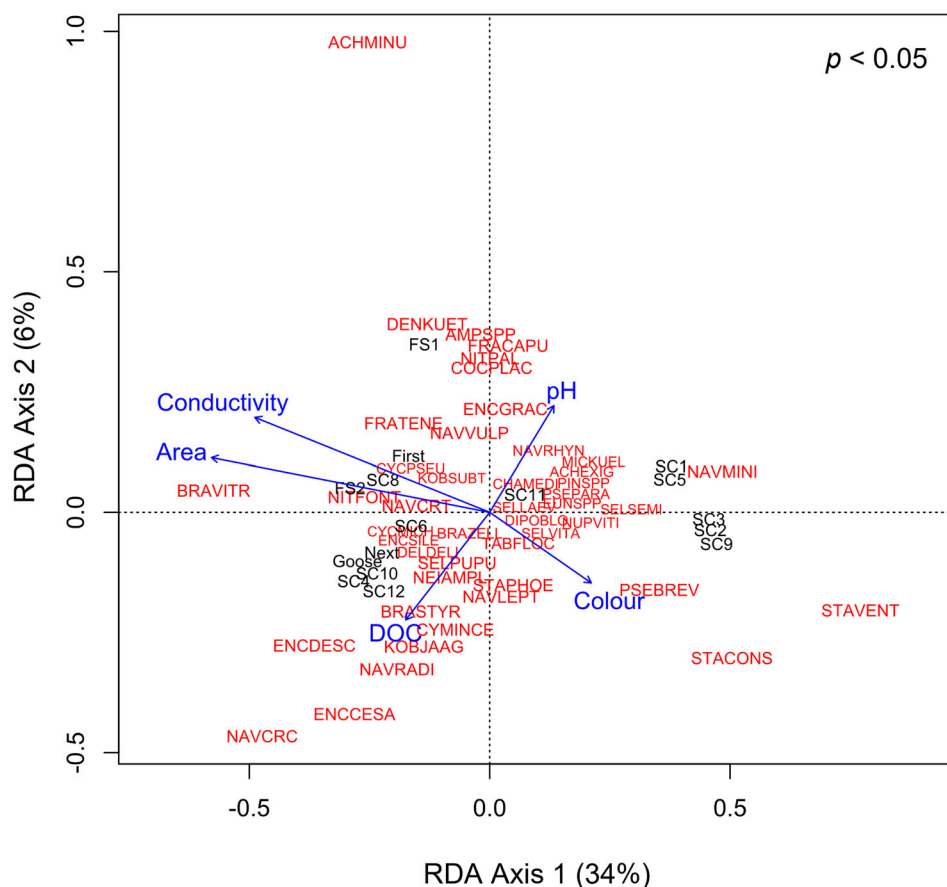


Figure 6. Redundancy analysis (RDA) ordination triplot illustrating relationships between diatom species and environmental variables, represented by arrows. Lake sites are in black. Diatoms species codes (red) are listed in [Supplemental Material](#).

consisted of large *Navicula* spp., *Encyonopsis* spp., and *Brachysira* spp. (*B. striata* and *B. vitrea*; [Table 3](#)). Chrysophyte cyst abundances were generally low in the substrate samples (2–6%), except for submerged peat, which had higher abundances (26%). Protozoan plates were almost entirely absent in these samples (~0–0.25%; [Table 3](#)).

Discussion

The peatland-dominated Scotty Creek basin is in a period of rapid transition due to climate warming and rapid loss of permafrost. The aim of this study was to characterize the present-day limnology and ecology of shallow lakes in or near Scotty Creek and underlying drivers as a benchmark to study future change. Spatial patterns in water chemistry, lake physical characteristics, and diatom assemblages were explored in 16 lakes. For 9 of the 16 lakes where landscape classification data were available, the extent of fen and collapse scar coverage was explored as a driver of water chemistry. Lastly, loggers were

deployed in First Lake and Goose Lake to gain a better understanding of seasonal dynamics in water depth, temperature, and oxygen.

Seasonal dynamics in Goose Lake and First Lake

Goose Lake and First Lake did not exhibit thermal stratification over the 76-day period the loggers were deployed. Paleolimnological records indicate that thermal stability has been increasing in lakes across the circumpolar Arctic in response to climate change (Rühland et al. 2015). Although stratification of shallow lakes is rare, it has been observed in shallow lakes with high DOC concentrations because DOC can absorb more solar radiation and increase surface water temperatures (Bouchard et al. 2011, Deshpande et al. 2017). Shallow boreal lakes may also be more prone to periodic thermal stratification where trees provide shelter from wind mixing (Klaus et al. 2021).

Oxygen availability at the sediment–water interface is a fundamental control on lake biogeochemical cycling. For example, methanogenesis, the production



Figure 7. Ground-level photographs of wetland sites and corresponding list of dominant diatom species identified in a sample retrieved from the site. Percentage of chrysophyte cysts and protozoan plates, in relation to diatom valves, are also listed.

of methane as a respiratory byproduct, occurs in anoxic conditions and may be fueled by the addition of terrestrial sources of organic carbon (Grasset et al. 2018). Increased stratification, in combination with increased bacterial consumption of high terrestrial carbon inputs, has resulted in prolonged periods of anoxia in some subarctic lakes in Northern Quebec (Deshpande et al. 2017). Small subarctic lakes in Norway similarly experienced decreasing oxygen concentrations with increasing DOC inputs (Couture et al. 2015). These changes could have important consequences for the carbon cycle as increased export of terrestrial carbon and longer periods of stratification may result in shallow subarctic lakes becoming important emitters of methane (Grasset et al. 2018). By contrast, high DOC subarctic lakes in Siberia had oxygen concentrations at equilibrium with the atmosphere (Shirokova et al. 2013). Oxygen levels near the sediment-water interface in Goose Lake and First Lake ranged between 5 and 12.5 mg/L and would be considered low for the protection of aquatic life (for reference,

9.5 mg/L is considered the lowest acceptable DO concentration for early life stages; CCME 1999). Because both Goose Lake and First Lake have high DOC concentrations (23.74 and 21.93 mg/L, respectively), high rates of microbial respiration may be responsible for lower oxygen levels because no evidence of stratification was found.

Peatlands cover ~19% of the circumpolar permafrost region (Tarnocai et al. 2009), yet high resolution limnological data of these sites are scarce and present a notable gap in global lake monitoring networks such as the Global Lakes Ecological Observation Network (GLEON). Because permafrost wetland complexes near the southern extent of permafrost are particularly vulnerable to rising air temperatures, the Scotty Creek basin offers an ideal location for long-term limnological research. Lake monitoring data collected can be combined with ongoing field, remote sensing, and modeling research at the Scotty Creek Research Station to provide a more holistic understanding of changes in terrestrial-aquatic linkages with permafrost thaw.

Table 3. Dominant diatom species identified in lake substrate samples.

	Sediment	Submerged peat	Grasses	Submerged vegetation	Benthic moss mat
Location	Shoreline	Shoreline	Shoreline	Shoreline	~1 m depth, north basin
Dominant diatoms	Large <i>Navicula</i> (~38%) Planktonic <i>Fragilaria</i> (~9%) <i>Encyonema</i> spp. (~8%) <i>Brachysira</i> (~7%)	Large <i>Navicula</i> (~30%) <i>Tabellaria</i> spp. (~11%) Planktonic <i>Fragilaria</i> (~9%) <i>Encyonopsis</i> spp. (~9%)	<i>Tabellaria</i> spp. (~48%) <i>Gomphonema</i> spp. (~21%) <i>Achnantheidium minutissimum</i> (~11%)	<i>Tabellaria</i> spp. (~71%)	Large <i>Navicula</i> spp. (~39%) <i>Encyonopsis</i> spp. (~14%) <i>Brachysira</i> spp. (~11%) <i>Achnanthes</i> spp. (~10%)
Cysts	Cysts (%): 4%	Cysts (%): 26%	Cysts (%): 2%	Cysts (%): 2%	Cysts (%): 6%
Protozoan plates	Plates (%): 0.24%	Plates (%): 0%	Plates (%): 0%	Plates (%): 0%	Plates (%): 0.25%

Percentage of chrysophyte cysts and protozoan plates, in relation to diatom valves, also included.

Spatial patterns in lake water chemistry

We expected the relative proportion of collapse scars and channel fens within 250 m of the lake shoreline to be an important driver of water chemistry in the Scotty Creek basin because of the differential roles these landscape features play in the biogeochemical processing and transport of materials from land to lake. In this landscape, channel fens act as water conveyors while collapse scars act predominately as water storage (Quinton et al. 2019). Collapse scars may be important sources of chromophoric DOC because they were identified in this study as having high DOC and high color (522 TCU). Our spatial results, however, showed limited evidence for the role of channel fens and collapse scars in driving lake water chemistry. For example, SC5 and SC8 were hydrologically isolated from the channel fen network, and both had high color, which may suggest that channel fens have a role in flushing terrestrial DOC from lakes; however, Next Lake also had relatively high color despite being well connected hydrologically.

We postulate that temporal dynamics in a rapidly changing landscape could explain why we found no strong spatial evidence for the importance of fen and collapse scar extent in influencing lake water chemistry. For example, an increase in fen development could initially increase color in lakes because of a phenomenon known as “bog capture” (Connon et al. 2014), where previously isolated collapse scar wetlands become connected to the expanding fen network as permafrost plateaus continue to degrade. The highly colored water is then conveyed to nearby lakes through the fen network. With time, colored DOC may ultimately be flushed from Next Lake and other lakes recently influenced by the capture of collapse scars. Paleolimnological approaches that reconstruct DOC trajectories in lakes in combination with a time series of remotely sensed images could be used in future studies to test this possibility.

Diatom ecology in permafrost wetlands and lakes of the Scotty Creek basin

Two different diatom assemblages were observed in 13 of the 16 lakes sampled. The first assemblage, identified in 6 lakes, was composed of small benthic *Fragilariaceae* and small *Navicula* species (*sensu lato*), which were found in this study to be associated with higher color. A similar assemblage was identified in a lake with high color located southeast of the Scotty Creek basin near Tathlina Lake (Coleman et al. 2015, Korosi et al. 2015). Small benthic *Fragilariaceae* have been used as indicators of harsher, low light conditions and tend to decrease in abundance with warming (Bouchard et al. 2013, Rühland et al. 2015). Although primarily benthic, they have also been identified as tychoplanktonic (e.g., Velez et al. 2021) and can be displaced into the water column with mixing; however, their absence in Goose Lake and First Lake, which seemed to be well mixed at least during the ice-free season of 2019, suggests that their presence is not related primarily to column mixing.

The second assemblage, recorded in 7 lakes, was composed of *Encyonopsis* spp. and large *Navicula* spp., which were found to be associated with high DOC and lower pH (although note the pH gradient is narrow, ranging from 7.85 to 8.75). The species assemblages in these lakes were similar to the assemblage found in the benthic moss mat sampled from Goose Lake. While large *Navicula* species have been associated with higher DOC (Rühland et al. 2003, Coleman et al. 2015), *Encyonopsis* species are epiphytic and often associated with mosses (Bahls 2013). Therefore, a main driver of diatom assemblages in these lakes may be the presence of a benthic moss mat, which is dependent on light penetrating to the benthic zone of these lakes. Colored DOC could have limited the growth of moss and associated epiphytes in these lakes. DOC has previously been shown to negatively impact benthic primary production in boreal lakes in Sweden and Alaska

through light limitation (Seekell et al. 2015), although the study did not distinguish between DOC and lake color, and aquatic plants are known to produce autochthonous, non-chromophoric DOC (Pagano et al. 2014). We infer autochthonous DOC sources from extensive moss and macrophyte growth to be the reason why our diatom epiphyte-dominated lakes exhibited high DOC but were generally lower in color. A better understanding of the interplay between lake depth, DOC, light, and benthic primary production is needed to predict the consequences of permafrost thaw on shallow lakes in boreal permafrost peatlands.

The species assemblages present in high abundances in wetlands were different from assemblages identified in lakes. Three of the most common species or groups of species were *Eunotia* spp., *Gomphonema* spp., and *Tabellaria* spp. *Eunotia* spp. in particular are commonly identified in paleoecological studies using peat cores and have lower pH optima (e.g., Hargan et al. 2015). *Tabellaria* spp. has been found in a wide variety of freshwater habitats, including lakes and peatlands, and has broad morphological variations in terms of size, but shorter species/varieties as found here have often been observed in peatlands and attached to vegetation (DeColibus 2013). This finding is consistent with the assemblages identified in the substrate samples where *Tabellaria* spp. was found in high abundances in grasses and submerged vegetation. The diatom assemblage identified in the collapse scar site was found to be different from both lakes and fens and was dominated by *K. subtilissima* (95%). Hargan et al. (2015) also found that *K. subtilissima* had higher prevalence in collapse scar habitats. Collapse scars also had the highest abundance of cysts and protozoan plates compared to both fens and lakes.

The 2 different assemblages of diatoms identified in these shallow subarctic lakes are likely driven by relative differences in benthic to pelagic production, which is impacted by the ability of light to penetrate the water column. Because increasing colored DOC concentrations can reduce light penetration, paleolimnological studies using diatoms as paleoindicators may be useful for examining the trajectory of lake browning with continued permafrost thaw. The low abundances of common wetland species also identified in lakes suggests we are not seeing a strong biological signal of these environments in the lakes. We can therefore be confident that the diatom assemblages recorded in lakes are indicative of that lake's conditions and have not been transported from other locations. Note, however, that changing lake depth and duration of the ice-free season may also influence the relative importance of benthic to

pelagic production in lakes, and decreases in lake depth are expected with drying of wetlands with ongoing thaw and loss of permafrost (Chasmer and Hopkinson 2017, Carpino et al. 2021). This finding highlights the importance of continued high-resolution monitoring in addition to paleolimnological studies to better predict how these lakes will change with future warming in this dynamic landscape.

Summary of main findings and future directions

The Scotty Creek basin is experiencing a rapid loss of permafrost that manifests as wetland thermokarst, where ground subsidence results in the conversion of black spruce forest into wetlands and enhances watershed hydrological connectivity (Quinton et al. 2019). Given the differing roles that forested peat plateaus, channel fens, and collapse scars play in the transport and processing of DOC, we predicted that the degree of lake connection to the channel fen network could be related to lake chromophoric DOC, but this hypothesis was not supported by our data. DOC and lake color, however, do seem to be key drivers of diatom assemblages in these lakes, with diatom assemblages tending to fall into 1 of 2 clusters. One cluster, composed of small benthic Fragilariaceae and small *Navicula* spp. (sensu lato), was found associated with higher lake color while the second cluster was composed of epiphytic *Encyonopsis* and large *Navicula* spp. and was associated with high DOC, lower color, and the presence of a benthic moss mat. Future directions should explore DOC quality (and its drivers) in these lakes and the interplay among DOC, lake depth, and light in structuring diatom assemblages and benthic primary production. Furthermore, because Scotty Creek is already in a period of rapid transition, long-term studies are needed to understand the trajectories and mechanisms of limnological change. First Lake and Goose Lake present ideal candidate sites for the establishment of a long-term limnological monitoring program, and the close association between diatoms and lake DOC/color indicate that diatoms will be useful paleoecological indicators of changes in lake carbon and primary production dynamics in future studies.

Acknowledgements

We thank Arnab Shuvo for assistance in the field, Kristine Haynes and Mason Dominico for providing precipitation data, and Emily Stewart for reviewing this manuscript and providing advice. Scotty Creek is within the traditional territory of the Łı́ıłłı́ Kúę First Nation (LKFN). Mahsi to the

LKFN and the Dehcho First Nations for their support and leadership in scientific research at Scotty Creek.

Disclosure statement

No potential conflict of interest was reported by the author(s).

Funding

This research was supported by a Natural Sciences and Engineering Research Council of Canada (NSERC) Discovery and Northern Supplement to JBK, and an NSERC postgraduate scholarship and Weston Family Foundation scholarship to KAC. Fieldwork funding and logistical support was also provided by ArcticNet, the Polar Continental Shelf Program, and the Northern Scientific Training Program.

ORCID

Kristen A. Coleman  <http://orcid.org/0000-0003-1876-3666>

Data Availability

Data associated with this manuscript are available through the York University Yorkspace Institutional Repository at <http://hdl.handle.net/10315/39723>.

References

- [APHA] American Public Health Association. 1998. Standard methods for the examination of water and wastewater. 20th ed. Washington (DC): American Public Health Association, American Water Works Association and Water Environmental Federation.
- [APHA] American Public Health Association. 2011. Standard methods for the examination of water and wastewater. 22nd ed. Washington (DC): American Public Health Association.
- Bahls L. 2013. *Encyonopsis* from western North America: 31 species from Alberta, Idaho, Montana, Oregon, South Dakota, and Washington, including 17 species described as new. Northwest diatoms, Volume 5. Helena (MT): The Montana Diatom Collection; 46 p.
- Battarbee RW, Jones VJ, Flower RJ, Cameron NG, Bennion H, Carvalho L, Juggins S. 2001. Diatoms. In: Smol JP, Birks HJB, Last WM, editors. Tracking environmental change using lake sediments, vol. 3: Terrestrial, algal, and siliceous indicators. Dordrecht (Netherlands): Kluwer Academic Press; p. 155–202.
- Bouchard F, Francus P, Pienitz R, Laurion I. 2011. Sedimentology and geochemistry of thermokarst ponds in discontinuous permafrost, subarctic Quebec, Canada. J Geophys Res Biog. 116(G2):1–14.
- Bouchard F, Pienitz R, Ortiz JD, Francus P, Laurion I. 2013. Palaeolimnological conditions inferred from fossil diatom assemblages and derivative spectral properties of sediments in thermokarst ponds of subarctic Quebec, Canada. Boreas. 42:575–595.
- Carpino O, Haynes K, Connon R, Craig J, Devoie É, Quinton W. 2021. Long-term climate-influenced land cover change in discontinuous permafrost peatland complexes. Hydrol Earth Syst Sci. 25(6):3301–3317.
- [CCME] Canadian Council of Ministers of the Environment. 1999. Canadian water quality guidelines for the protection of aquatic life: dissolved oxygen (freshwater). In: Canadian environmental quality guidelines. Winnipeg (MB): Canadian Council of Ministers of the Environment.
- Chasmer L, Hopkinson C, Veness T, Quinton W, Baltzer J. 2014. A decision-tree classification for low-lying complex land cover types within the zone of discontinuous permafrost. Remote Sens Environ. 143:73–84.
- Chasmer L, Hopkinson C. 2017. Threshold loss of discontinuous permafrost and landscape evolution. Glob Change Biol. 23(7):2672–2686.
- Cole JJ, Carpenter SR, Pace ML, Van de Bogert MC, Kitchell JL, Hodgson JR. 2006. Differential support of lake food webs by three types of terrestrial organic carbon. Ecol Lett. 9:558–568.
- Cole JJ, Prairie YT, Caraco NF, McDowell WH, Tranvik LJ, Striegl RG, Duarte CM, Kortelainen P, Downing JA, Middelburg JJ, Melack J. 2007. Plumbing the global carbon cycle: integrating inland waters into the terrestrial carbon budget. Ecosystems. 10:172–185.
- Coleman KA, Korosi JB. 2023. Dataset: (Paleo)limnological data for small, shallow lakes at or near the Scotty Creek Research Station in the Dehcho region (Northwest Territories, Canada). <http://hdl.handle.net/10315/39723>
- Coleman KA, Palmer MJ, Korosi JB, Kokelj SV, Jackson K, Hargan KE, Courtney Mustaphi CJ, Thienpont JR, Kimpe LE, Blais JM, et al. 2015. Tracking the impacts of recent warming and thaw of permafrost peatlands on aquatic ecosystems: a multi-proxy approach using remote sensing and lake sediments. Boreal Environ Res. 20:363–377.
- Connon RF, Quinton WL, Craig JR, Hayashi M. 2014. Changing hydrologic connectivity due to permafrost thaw in the lower Liard River valley, NWT, Canada. Hydrol Process. 28:4163–4178.
- Couture RM, de Wit HA, Tominaga K, Kiuru P, Markelov I. 2015. Oxygen dynamics in a boreal lake responds to long-term changes in climate, ice phenology, and DOC inputs. J Geophys Res Biogeosci. 120:2441–2456.
- DeColibus D. 2013. *Tabellaria flocculosa*. In: Diatoms of North America. https://diatoms.org/species/tabellaria_flocculosa
- Deshpande BN, Maps F, Matveev A, Vincent WF. 2017. Oxygen depletion in subarctic peatland thaw lakes. Arctic Sci. 1:1–23.
- Fallu MA, Allaire N, Pienitz R. 2002. Distribution of freshwater diatoms in 64 Labrador (Canada) lakes: species-environment relationships along latitudinal gradients and reconstruction models for water color and alkalinity. Can J Fish Aquat Sci. 59:329–349.
- Frey KE, McClelland JW. 2009. Impacts of permafrost degradation on arctic river biogeochemistry. Hydrol Process. 23(1):169–182.
- Glew JR. 1988. A portable extruding device for close interval sectioning of unconsolidated core samples. J Paleolimnol. 1(3):235–239.
- Gordon J, Quinton W, Branfireun BA, Olefeldt D. 2016. Mercury and methylmercury biogeochemistry in a thawing

- permafrost wetland complex, Northwest Territories, Canada. *Hydrol Process.* 30:3627–3638.
- Grasset C, Mendonça R, Villamor Saucedo G, Bastviken D, Roland F, Sobek S. **2018.** Large but variable methane production in anoxic freshwater sediment upon addition of allochthonous and autochthonous organic matter. *Limnol Oceanogr.* 63(4):1488–1501.
- Guiry MD, Guiry GM. **2021.** AlgaeBase. World-wide electronic publication, National University of Ireland, Galway. <https://www.algaebase.org>
- Hargan KE, Rühland KM, Paterson AM, Finkelstein SA, Holmquist JR, MacDonald GM, Keller W, Smol JP. **2015.** The influence of water-table depth and pH on the spatial distribution of diatom species in peatlands of the Boreal Shield and Hudson Plains, Canada. *Botany.* 93:57–74.
- Harrell FE. **2021.** Hmisc: Harrell miscellaneous. R package version 4.5-0. <https://CRAN.R-project.org/package=Hmisc>
- Harris LI, Richardson K, Bona KA, Davidson SJ, Finkelstein SA, Garneau M, McLaughlin J, Nwaishi F, Olefeldt D, Packalen M, Roulet NT. **2022.** The essential carbon service provided by northern peatlands. *Front Ecol Environ.* 20:222–230.
- Hugelius G, Loisel J, Chadburn S, Jackson RB, Jones M, MacDonald G, Marushchak M, Olefeldt D, Packalen M, Siewert MB, Treat C. **2020.** Large stocks of peatland carbon and nitrogen are vulnerable to permafrost thaw. *Proc Natl Acad Sci.* 117:20438–20446.
- Ivanov K, Zaprianova P, Petkova M, Stefanova V, Kmetov V, Georgieva D, Angelova V. **2012.** Comparison of inductively coupled plasma mass spectrometry and colorimetric determination of total and extractable phosphorus in soils. *Spectrochimica Acta Part B: At Spectrosc.* 71-72:117–122.
- Karlsson JM, Lyon SW, Destouni G. **2012.** Thermokarst lake, hydrological flow and water balance indicators of permafrost change in Western Siberia. *J Hydrol.* 464–465:459–466.
- Kettles I, Tarnocai C. **1999.** Development of a model for estimating the sensitivity of Canadian peatlands to climate warming. *Geogr Phys Quatern.* 53(3):323–338.
- Klaus M, Karlsson J, Seekell D. **2021.** Tree line advance reduces mixing and oxygen concentrations in arctic-alpine lakes through wind sheltering and organic carbon supply. *Glob Change Biol.* 27:4238–4253.
- Korosi JB, McDonald J, Coleman KA, Palmer MJ, Smol JP, Simpson MJ, Blais JM. **2015.** Long-term changes in organic matter and mercury transport to lakes in the sporadic discontinuous permafrost zone related to peat subsidence. *Limnol Oceanogr.* 60(5):1550–1561.
- Krammer K, Lange-Bertalot H. **1997.** Bacillariophyceae 2. Teil: Bacillariaceae, Epithemiaceae, Surirellaceae. Süßwasserflora von Mitteleuropa 2/2. Berlin (Germany): Spektrum Akademischer Verlag.
- Krammer K, Lange-Bertalot H. **1999.** Bacillariophyceae 1. Teil: Naviculaceae. Süßwasserflora von Mitteleuropa 2/1. Berlin (Germany): Spektrum Akademischer Verlag.
- Krammer K, Lange-Bertalot H. **2000.** Bacillariophyceae 3. Teil: Centrales, Fragilariaceae, Eunotiaceae. Süßwasserflora von Mitteleuropa 2/3. Berlin (Germany): Spektrum Akademischer Verlag.
- Mack M, Connors R, Makarieva O, McLaughlin J, Nesterova N, Quinton W. **2021.** Heterogenous runoff trends in peatland-dominated basins throughout the circumpolar North. *Environ Res Comms.* 3:075006.
- Oksanen J, Blanchet FG, Friendly M, Kindt R, Legendre P, McGlinn D, Minchin PR, O'hara RB, Simpson GL, Solymos P, Stevens MHH. **2019.** vegan: Community Ecology Package (version 2.5-6). The Comprehensive R Archive Network.
- O'Neill HB, Wolfe SA, Duchesne C. **2019.** New ground ice maps for Canada using a paleogeographic modelling approach. *Cryosphere.* 13:753–773.
- Pagano T, Bida M, Kenny J. **2014.** Trends in levels of allochthonous dissolved organic carbon in natural water: a review of potential mechanisms under a changing climate. *Water.* 6:2862–2897.
- Porcal P, Koprivnjak JF, Molot LA, Dillon PJ. **2009.** Humic substances—part 7: the biogeochemistry of dissolved organic carbon and its interactions with climate change. *Environ Sci Pollut Res.* 16:714–726.
- Quinton W, Berg A, Braverman M, Carpino O, Chasmer L, Connors R, Craig J, Devoie É, Hayashi M, Haynes K, Olefeldt D. **2019.** A synthesis of three decades of hydrological research at Scotty Creek, NWT, Canada. *Hydrol Earth Syst Sci.* 23(4):2015–2039.
- R Core Team. **2020.** R: a language and environment for statistical computing. Vienna(Austria): R foundation for Statistical Computing.
- Rühland K, Paterson AM, Smol JP. **2015.** Diatom assemblage responses to warming: reviewing the evidence. *J Paleolimnology.* 54:1–35.
- Rühland K, Priesnitz A, Smol JP. **2003.** Paleolimnological evidence from diatoms for recent environmental changes in 50 lakes across Canadian Arctic treeline. *Arct Antarct Alp Res.* 35(1):110–123.
- Seekell DA, Lapierre JF, Ask J, Bergström AK, Deininger A, Rodriguez P, Karlsson J. **2015.** The influence of dissolved organic carbon on primary production in northern lakes. *Limnol Oceanogr Lett.* 60(4):1276–1285.
- Shirokova LS, Pokrovsky OS, Kirpotin SN, Desmukh C, Pokrovsky BG, Audry S, Viers J. **2013.** Biogeochemistry of organic carbon, CO₂, CH₄, and trace elements in thermokarst water bodies in discontinuous permafrost zones of Western Siberia. *Biogeochemistry.* 113:573–593.
- Sim TG, Swindles GT, Morris PJ, Baird AJ, Cooper CL, Gallego-Sala AV, Charman DJ, Roland TP, Borken W, Mullan DJ, Aquino-Lopez MA. **2021.** Divergent responses of permafrost peatlands to recent climate change. *Environ Res Lett.* 16:034001.
- Smith LC, Pavelsky TM, MacDonald GM, Shiklomanov AI, Lammers RB. **2007.** Rising minimum daily flows in northern Eurasian rivers: a growing influence of groundwater in the high-latitude hydrologic cycle. *J Geophys Res Biogeosci.* 112:1–18.
- [SOCR] State of the Cryosphere Report. **2021.** A needed decade of urgent action. www.iccinet.org/statecryo21
- Spaulding SA, Potapova MG, Bishop IW, Lee SS, Gasperak TS, Jovanoska E, Furey PC, Edlund MB. **2021.** Diatoms.org: supporting taxonomists, connecting communities. *Diatom Res.* 36(4):291–304.
- Spence C, Norris M, Bickerton G, Bonsal BR, Brua R, Culp JM, Dibike Y, Gruber S, Morse PD, Peters DL, Shrestha R. **2020.** The Canadian water resource vulnerability index to permafrost thaw (CWRVIPT). *Arctic Sci.* 6(4):437–462.

- Tanentzap AJ, Kielstra BW, Wilkinson GM, Berggren M, Craig N, Del Giorgio PA, Grey J, Gunn JM, Jones SE, Karlsson J, et al. **2017**. Terrestrial support of lake food webs: synthesis reveals controls over cross-ecosystem resource use. *Sci Adv.* 3:e1601765.
- Tank SE, Vonk JE, Walvoord MA, McClelland JW, Laurion I, Abbott BW. **2020**. Landscape matters: predicting the biogeochemical effects of permafrost thaw on aquatic networks with a state factor approach. *Permafr Periglac Process.* 31:358–370.
- Tarnocai C, Canadell CJG, Schuur EAG, Kuhry P, Mazhitova G, Zimov S. **2009**. Soil organic carbon pools in the northern circumpolar permafrost region. *Glob Biogeochem Cycles.* 23:GB2023.
- Thienpont JR, Rühland KM, Pisarcic MF, Kokelj SV, Kimpe LE, Blais JM, Smol JP. **2013**. Biological responses to permafrost thaw slumping in Canadian Arctic lakes. *Freshw Biol.* 58:337–353.
- Velez MI, Salgado J, Brenner M, Hooghiemstra H, Escobar J, Boom A, Bird B, Curtis JH, Temoltzin-Loranca Y, Patino LF, Gonzalez-Arango C. **2021**. Novel responses of diatoms in neotropical mountain lakes to indigenous and post-European occupation. *Anthropocene.* 34:1–13.
- Vonk JE, Alling V, Rahm L, Mörtz CM, Humborg C, Gustafsson Ö. **2012**. A centennial record of fluvial organic matter input from the discontinuous permafrost catchment of Lake Torneträsk. *J Geophys Res Biogeosci.* 117(G3):1–11.
- Vonk JE, Mann PJ, Davydov S, Davydova A, Spencer RGM, Schade J, Sobczak WV, Zimov N, Zimov S, Bulygina E, et al. **2013**. High biolability of ancient permafrost carbon upon thaw. *Geophys Res Lett.* 40:2689–2693.
- Vonk JE, Tank SE, Bowden WB, Laurion I, Vincent WF, Alekseychik P, Amyot M, Billet MF, Canario J, Cory RM, Deshpande BN. **2015**. Reviews and syntheses: effects of permafrost thaw on Arctic aquatic ecosystems. *Biogeosciences.* 12(23):7129–7167.
- Vonk JE, Tank SE, Walvoord MA. **2019**. Integrating hydrology and biogeochemistry across frozen landscapes. *Nat Comm.* 10:1–4.
- Wauthy M, Rautio M, Christoffersen KS, Forsström L, Laurion I, Mariash HL, Peura S, Vincent WF. **2018**. Increasing dominance of terrigenous organic matter in circumpolar freshwaters due to permafrost thaw: increasing allochthony in arctic freshwaters. *Limnol Oceanogr Lett.* 3:186–198.
- Wickham H, Averick M, Bryan J, Chang W, McGowan L, François R, Grolemond G, Hayes A, Henry L, Hester J, et al. **2019**. Welcome to the tidyverse. *J Open Source Soft.* 4(43):1686.
- Zhang T, Barry RG, Knowles K, Heginbottom JA, Brown J. **1999**. Statistics and characteristics of permafrost and ground ice distribution in the Northern Hemisphere. *Polar Geogr.* 23(2):132–154.
- Zhang TJ, Frauenfeld OW, Serreze MC, Etringer A, Oelke C, McCreight J, Barry RG, Gilichinsky D, Yang DQ, Ye HC, et al. **2005**. Spatial and temporal variability in active layer thickness over the Russian Arctic drainage basin. *J Geophys Res Atmospheres.* 110:D16101.